

The Spectrum of SnF

F. A. JENKINS AND GEORGE D. ROCHESTER*

Department of Physics, University of California, Berkeley, California

(Received September 24, 1937)

Measurements of the absorption bands of SnF are reported for the first time. Analysis of the frequencies of the band heads shows the presence of four doublet systems, all due to transitions from a doublet normal state X , of separation 2317.3 cm^{-1} . The various states are as follows:

STATE	ν	ω_e	$x_e\omega_e$	PROBABLE TYPE
X	0.0	582.9	2.69	$^2\Pi$
	2317.3	587.6	2.65	
A	34,108.4	676.7	2.65	$^2\Sigma$
B	40,834	594	—	$^2\Delta$
C	44,161.6	688.2	4.65	$^2\Pi$
	45,498.9	688.2	4.65	
D	46,326	598	—	$^2\Delta$
	46,427	607	—	
E	$\sim 41,000$	—	—	—
F	$\sim 53,000$	—	—	—

The transitions $E \leftarrow X$ and $F \leftarrow X$ give continua. The second component of $B \leftarrow X$ is probably masked by $E \leftarrow X$. Resolution of the Sn isotope effect is observed for the first time. A carbon tube furnace for studying absorption spectra is described.

THIS is the first of a series of investigations of the ultraviolet absorption spectra of the heavy metal halides under high dispersion. Plates have already been obtained for a number of these, using a newly constructed carbon tube furnace, and a 30,000 line/in. aluminum grating of 21 foot radius which permits the ultraviolet spectrum to be studied as far as the limit of transmission of air. The fluorides are the most satisfactory for investigating the nature of the electronic states involved, not only because of their smaller moment of inertia, but also because of their freedom from the isotope effect which complicates the chloride spectra.

EXPERIMENTAL

The furnace used for vaporizing the salts proved to be unusually efficient and convenient. As shown in Fig. 1, it is of the "cartridge" type, in which the large cylindrical vacuum chamber can be rolled away from the end plate,

* Commonwealth Fund Fellow. Now at the University of Manchester, England.

on which the carbon tube and its various heat shields are rigidly mounted. Since the heated portion is almost entirely surrounded by a water-jacket, a rubber gasket can be used for the vacuum seal. The heating element A is a graphite tube 12 in. long, of $\frac{1}{2}$ in. internal diameter, and wall thickness $\frac{3}{32}$ in. This is tightly wedged in at the ends by the tapered graphite blocks F, F bearing on water-cooled copper surfaces. Surrounding it is a graphite tube B which acts as the primary heat shield. Immediately outside this is an iron tube C perforated around its circumference by a row of holes near its junction to the end plate. This reduces loss of heat by conduction. The water jacket E is made from two brass cylinders with a clearance of only $\frac{1}{16}$ in. between them. The space D is packed with loosely fitting sheets of molybdenum, which greatly increase the efficiency of the heat shielding. The current leads are two heavy copper tubes with internal water cooling. Insulation of one of these leads, and of the main water jacket, from the end plate is accomplished by

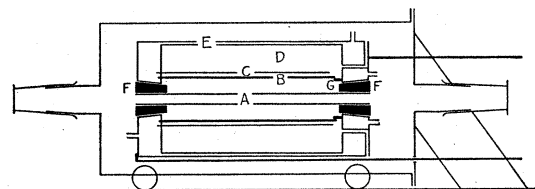


FIG. 1. Schematic diagram of furnace.

mica washers. The end of the graphite tube *B* is held in place by a lavite ring *G*.

The current is supplied at 15 or 20 volts by a large transformer. Temperatures were measured

with an optical pyrometer, and preliminary trials showed that a temperature of 2000°C required a power of 9.1 kva, excluding transformer losses. For the present work it was found best to fill the furnace with nitrogen at atmospheric pressure to prevent diffusion of the fluoride vapor to the quartz windows.

The vapor of SnF was produced by heating equal parts of lead fluoride and metallic tin in a shallow graphite boat placed at the center of the heated tube. The source was a discharge through hydrogen at a pressure of 1 cm in a

TABLE I. Band heads of SnF.

A←X SYSTEM. HIGH FREQUENCY COMPONENT.										
ν' \ ν''	0	1	2	3	4	5	6	7	8	9
0	34,155.3	33,577.6	33,005.3							
	144.8	568.1	32,996.6							
1	34,826.6	34,249.2	33,676.0	33,110.6						
	815.7	239.1	667.9	101.6						
2	35,493.0			33,777.2	—					
	481.0			768.5	33,208.1					
3	36,153.7	35,576.6	35,005.0			33,319.2				
	138.8	564.0	34,992.8			307.9				
4		36,232.8	35,661.0	35,094.2	34,533.5					
		219.4	649.2	084.0	524.3					
5	—	36,882.3	36,310.7	35,744.3	—	34,626.6				
	37,446.9	867.0	297.6	732.6	35,191.8	618.1				
6				36,389.6	35,827.1		34,721.3			
				376.4	814.6		711.9			
7				37,027.8	36,466.8	35,912.3		34,814.4		
				012.7	453.4	899.6				
8				37,100.8	36,544.1	35,993.7				
				085.8	531.9	981.5				
9						37,173.1	36,621.9	36,075.7		
						158.6	609.4			
10							37,244.3	36,699.3	36,158.4	
							230.4	687.7		
11								37,316.9	36,775.7	
								303.3		
12									37,388.6	36,852.3
									375.3	

A←X SYSTEM. LOW FREQUENCY COMPONENT.							B←X SYSTEM.			
ν' \ ν''	0	1	2	3	4	5	6	0	1	2
0	31,835.7	31,253.3	30,675.8					38,522.8	37,941.5	
	825.8	244.3	667.8					516.2	933.9	
1	32,507.4	31,925.7	31,347.9	30,775.9				39,116.7	—	37,965.9
	496.8	916.1	339.3	768.2				106.9	38,528.2	958.2
2	33,172.0	32,591.3		31,442.5	30,876.1				—	
	161.8	581.4		434.6	868.6				39,093.3	
3			32,675.4			30,973.9				
			664.9			965.6				39,067.3
4			33,331.6	32,760.2						
			319.2	750.0						
5						32,282.3				
						273.8				
6							32,372.3			
							362.3			

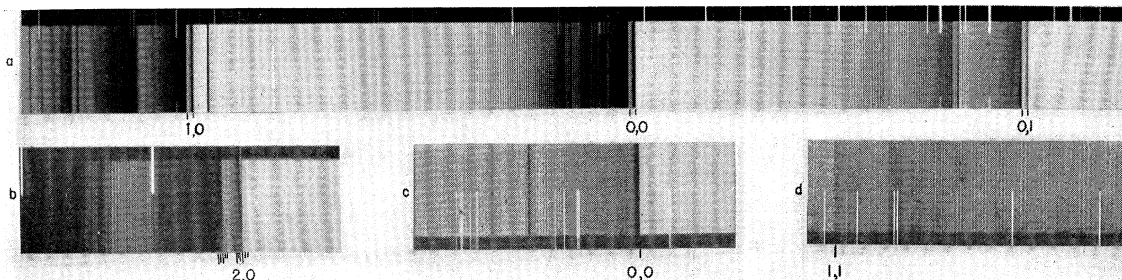


FIG. 2. (a) and (b) ${}^2\Sigma$, ${}^2\Pi$ system of SnF. (c) ${}^2\Pi$, ${}^2\Pi$ system of SnF. (d) V , N system of AgCl.

water cooled tube furnished with large aluminum electrodes in side tubes and having a quartz capillary of $2\frac{1}{2}$ mm internal diameter. With a current of 0.4 amp, suitably exposed plates were obtained from the grating in $\frac{1}{2}$ to 1 hour. Hilger Schumann plates were used in the region $\lambda\lambda 2000$ – 2600 , and Eastman 40 plates for $\lambda\lambda 2600$ – 3800 . The dispersion of the grating is 1.3 \AA/mm in this region of the first order. Three sets of plates were taken, at furnace temperature of 1320 , 1480 and 1740°C , in order to bring out the strong and weak parts of the spectrum with suitable intensity for measurement. Measurements were made of all band heads, and of a few rotational lines, against iron arc standards.¹

OBSERVATIONAL DATA

Whereas pure lead fluoride in the tube gave strong PbF bands, these are almost completely

suppressed by the introduction of tin, and practically all of the molecular absorption observed appears to be due to SnF. Altogether seven band systems are found, of which six are definitely associated in pairs to form three doublet systems of wide separation. In addition, two strong continua occur, and it is probable that the other doublet component of the odd seventh system is obscured by (or perhaps represented by) one of these continua. All observed bands are degraded toward the further ultraviolet, and with the exception of one system ($C\leftarrow X$) all have fairly close double heads. It will be convenient to discuss these systems separately.

System $A\leftarrow X$, $\lambda\lambda 2660$ – 3260

This is the most extensive system observed, and its strongest bands begin to appear at a

TABLE I.—(Continued).

C←X SYSTEM. HIGH FREQUENCY COMPONENT.						C←X SYSTEM. LOW FREQUENCY COMPONENT.		
v' \ v''	0	1	2	3	4	0	1	2
0	45,551.0	44,974.4	44,402.2			42,573.1		
1	46,228.9		45,080.9			42,240.7	42,661.1	
2	46,899.5	46,323.0			44,624.2		43,320.6	
3	47,560.3							43,403.0
D←X SYSTEM. HIGH FREQUENCY COMPONENT.					D←X SYSTEM. LOW FREQUENCY COMPONENT.			
v' \ v''	0	1	2	3	0	1	2	3
0	46,351.3	45,774.2			44,118.4	43,536.2		
	343.2	767.4			110.8	528.6		
1	46,959.2		45,809.2		44,715.2	44,133.7	43,555.3	
	950.0	46,374.7	802.7		706.4	125.5	548.7	
2	47,536.3			45,852.3		44,728.4		43,573.7
	526.1			844.2		719.9		567.8

¹ W. F. Meggers and C. J. Humphreys, Nat. Bur. Stand. J. Research **18**, 543 (1937).

TABLE II. *Calculated and observed isotope shifts.*

BAND	MOLECULE	ρ^{-1}	$\Delta\nu_{\text{calc}}$	$\Delta\nu_{\text{obs}}$ (P HEADS)	$\Delta\nu_{\text{obs}}$ (Q HEADS)
2,0	Sn ¹¹⁶ F	0.00235	3.02	2.8	2.7
	Sn ¹¹⁸ F	0.00116	1.53	1.4	1.2
	Sn ¹²⁰ F	0.00000	—	—	—
	Sn ¹²² F	-0.00112	1.58	1.6	1.4
	Sn ¹²⁴ F	-0.00221	3.22	3.2	3.0
1,0	Sn ¹²⁴ F	-0.00221	1.58	1.3	—
3,0	Sn ¹¹⁶ F	0.00235	4.73	—	4.7
	Sn ¹¹⁸ F	0.00116	2.33	—	2.3
4,1	Sn ¹¹⁶ F	0.00235	4.87	4.5	5.0
	Sn ¹¹⁸ F	0.00116	2.41	2.2	2.6
5,2	Sn ¹¹⁶ F	0.00235	5.03	—	5.1
	Sn ¹¹⁸ F	0.00116	2.49	2.5	2.5

furnace temperature of about 980°C. It consists of two electronic components, of separation 2317.3 cm⁻¹. The band structure and intensity distribution in the two components are exactly alike, but the high frequency component is much more intense. This shows that the doubling is in the lower state, and the observed ratio of intensities is consistent with the ratio 6 to 1 calculated from the Boltzmann factor for 1800°K.

Fig. 2(a) is an enlargement of the three strongest sequences as they are developed at 1600°C. Wave numbers of the band heads are given in Table I. The two values for each vibrational transition refer to the two heads, *P* and *Q*, observed for each band. The *Q* heads are represented by the equation

$$\nu = \left. \begin{array}{l} 34,108.4 \\ 31,791.1 \end{array} \right\} + 676.7u' - 2.65u'^2 - \left. \begin{array}{l} 582.9 \\ 587.6 \end{array} \right\} u'' + \left. \begin{array}{l} 2.69 \\ 2.65 \end{array} \right\} u''^2,$$

where $u = v + \frac{1}{2}$.

All heads except those of the 0,0 and 1,1 bands show evidence of the tin isotope effect. This is especially well resolved for the 2,0 band (Fig. 2(b)), where each head is split into five nearly equally spaced components, the two low frequency ones being much weaker than the other three. According to Aston, tin has 11 isotopes, but the above is just the pattern expected² when one takes into account only the

² A diagram of the predicted pattern is given by W. Jevons, Proc. Roy. Soc. 110A, 387 (1926).

more intense and favorably situated bands. Table II lists the observed and calculated isotope shifts for some of the more easily measured cases. For all bands on the short wave side of the system origin, the measurements of Table I refer to the first strong head, due to Sn¹²⁰F. For those on the long wave side, they probably represent Sn¹¹⁶F heads, but the isotope heads were not resolved on this side.

It was possible to measure a short series of structure lines between the *P* and *Q* heads of the 0,0 band in both components. These gave the same average second difference of 0.031 cm⁻¹, so that the value of $B' - B''$ is 0.015.

System $B \leftarrow X$, $\lambda\lambda 2556-2635$

This lies at the long wave end of the continuum $E \leftarrow X$ (see below), and is partly blotted out by it at the highest temperature. The vibrational constants are very nearly the same in the upper and lower states so that the bands in each sequence are very closely spaced. In fact, there appears to be a reversal in direction for the sequence $\Delta v = +1$. Under these conditions the band heads are a very poor representation of band origins, and there is little point in giving an equation for heads. Each band shows two heads, *P* and *Q*, with the *Q* head about half as intense as the *P*. Data for both are given in Table I, and indicate a value for $\Delta G_3'$ of about 594 cm⁻¹.

System $C \leftarrow X$, $\lambda\lambda 2100-2350$

The bands of this system (see Fig. 2(c)) have single heads, and the system as a whole is considerably less intense than those described above. It is about 1/10 as intense as the $D \leftarrow X$ system, which it overlies, and is well developed only at the highest temperature used. Only two sequences of the low frequency component could be found. This is presumably due to the others being masked by the $E \leftarrow X$ continuum. The *v* numbering for the observed bands is therefore somewhat uncertain, but that given in the table is indicated by both the intensity distribution in the sequences and by the ΔG values. There is a peculiar structure surrounding the two bands measured in the $\Delta v = +1$ sequence, consisting of what are apparently lines, band heads shaded in both directions, and regions of uniform absorp-

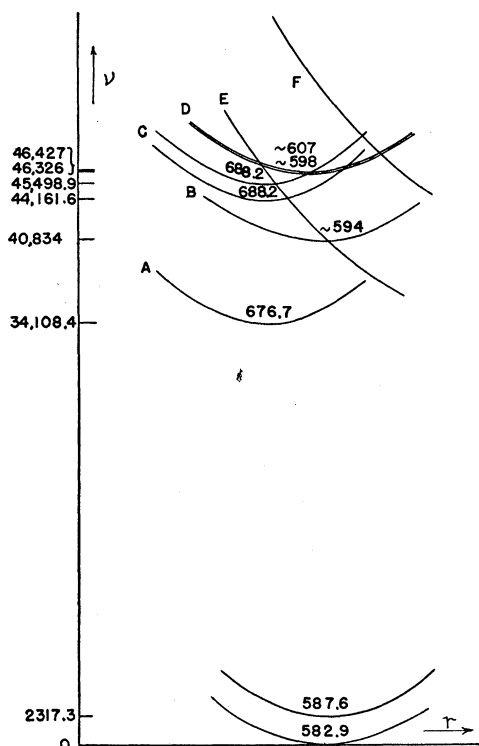


FIG. 3. Partial potential curves.

tion sharp on either edge. This is most likely due to strong perturbations. As in the case of the $A \leftarrow X$ bands, the low frequency component is much less intense. The heads of this system are given by the equations

$$\begin{aligned} \nu &= 45,498.9 + 688.2u' - 4.65u'^2 \\ &\quad - 582.9u'' + 2.69u''^2, \\ \nu &= 41,844.3 + 688.2u' - 4.65u'^2 \\ &\quad - 587.6u'' + 2.65u''^2. \end{aligned}$$

The lower states are therefore the same as those of the $A \leftarrow X$ system.

A fairly long series of rotational lines could be measured in the 0,0 band (Fig. 2(c)). They gave an average second difference of $2(B' - B'') = 0.067 \text{ cm}^{-1}$.

System $D \leftarrow X$, $\lambda\lambda 2060-2300$

This system is another wide doublet, with an intense high frequency component and a weak low frequency component. The bands are double headed, with the second head, or Q head, less intense. This difference in intensity is much

more marked in the low frequency component. The system as a whole is of about the same intensity as the $A \leftarrow X$ system. Above 1480°C it is entirely masked by the overlapping $F \leftarrow X$ continuum (see below). The values of ΔG from the matrix diagram (Table I) do not show good agreement. Evidently this results from the fact that the heads are far from the origins, as was the case with $B \leftarrow X$. The approximate values of $\Delta G_i'$ are 607 and 598 cm^{-1} for the high and low frequency systems, respectively. The discrepancy between these values probably has little significance.

The isotope effect is evident in this system, as well as in all others discussed above, from a diffuseness of the heads further removed from the system origin. In the case of the 1,0 head of the present system, the isotope structure was resolved, and the isotope shifts were measured as 1.3 and 1.2 cm^{-1} for Sn^{116}F and Sn^{124}F . These agree within the error of measurement with their computed values 1.47 and 1.38 cm^{-1} .

The continuous bands $E \leftarrow X$ and $F \leftarrow X$

These are two broad regions where the absorption is complete even at the lowest temperatures we used. Therefore all we can say about their intensity is that they are stronger than any of the discrete band systems. The width of the bands increases with temperature, and the approximate regions of absorption are as follows (estimated to half-absorption at either limit):

Temp.	$E \leftarrow X$	$F \leftarrow X$
1438°C	$\lambda\lambda 2370-2500$	-2010
1604	2360-2530	-2040
1860	2340-2580	-2300

It will be seen that the $F \leftarrow X$ continuum stretches toward short wave-lengths beyond the limit of observation, and that with increasing temperature it extends more rapidly toward long wave-lengths than does $E \leftarrow X$.

DISCUSSION

The spectrum of SnF should be analogous to the known spectra^{3,4} of SnCl and of PbF. In SnCl, two band systems and two continua are known. The normal state is a wide doublet of

³ W. Jevons, reference 2. Also W. F. C. Ferguson, Phys. Rev. **32**, 607 (1928).

⁴ G. D. Rochester, Proc. Roy. Soc. **153A**, 407 (1936).

separation 2360.1 cm^{-1} , and shows the characteristics of a ${}^2\Pi$ state. In SnF the situation must be similar, since we observe wide doublet systems whose separation is of the above order of magnitude. To evaluate this separation, we must consider the nature of the excited states. The two known⁵ excited states of SnCl are ${}^2\Delta$, at $28,665.3$ and $28,939.2 \text{ cm}^{-1}$, and ${}^2\Sigma$, at $33,622.6 \text{ cm}^{-1}$. The ${}^2\Sigma$ state is much more tightly bound ($\omega_e=431.3$) than the ${}^2\Delta$ ($\omega_e=297.5$, 296.2).

The lower parts of the potential curves for the various states of SnF are shown in Fig. 3, approximately as they must lie according to our interpretation of the data. The curvature at the minimum was calculated from the observed ω_e , and the relative values of r_e estimated from the relation $\omega_e r_e^2 = \text{const}$. It will be seen that of the two lowest excited states one is more tightly bound than the other. We interpret state *A* as being ${}^2\Sigma$, and state *B* as ${}^2\Delta$, even though the order of the states is interchanged from the case of SnCl. It is difficult to say whether the ${}^2\Delta$ state is inverted with respect to ${}^2\Pi$ or not, because in either case the second component would probably not be observed. If the observed *B*←*X* system is the high frequency component, the low frequency one would be much weaker and probably masked by the *A*←*X* bands. On the other hand, if it is the low frequency component, the other component would fall in the *E*←*X* continuum. In Fig. 3 we have assumed the latter to be true, because no trace has been found of a lower frequency component, and because the observed $\Delta G''$ values are more nearly those of the upper ${}^2\Pi$ component. Neither of these reasons is conclusive, however, and actually the relative intensities of the *P* and *Q* heads is more nearly that expected for the high

frequency component. A further reason for the above designation of states lies in the appearance of the bands. The *A*←*X* system resembles the ${}^2\Sigma\leftarrow{}^2\Pi$ system of SnCl. In both components the *Q* heads are about twice as strong as the *P* heads, as expected for this type of transition.

State *C* is unquestionably a second ${}^2\Pi$ state with a smaller doublet separation than that of the normal state. If the separation of the latter is taken as 2317.3 cm^{-1} from the *A*←*X* system, this upper ${}^2\Pi$ state must be inverted with respect to the lower one, with a splitting of 1337.3 cm^{-1} , since the observed separation of origins is 3654.6 cm^{-1} . This value is not too certain, however, for reasons mentioned earlier. The appearance of the bands is as expected for a ${}^2\Pi\leftarrow{}^2\Pi$ transition, since no evidence for a *Q* branch is present.

The bands of the *D*←*X* system have the appearance expected for a ${}^2\Delta\leftarrow{}^2\Pi$ transition. In particular, the lower relative intensity of the *Q* heads in the low frequency component⁶ points to this conclusion. The general appearance of the system is much the same as that in the ${}^2\Delta\leftarrow{}^2\Pi$ bands of SnCl. Hence we may identify state *D* as another ${}^2\Delta$. It is not inverted, since the observed separation is 2216 cm^{-1} , leaving 101 cm^{-1} for the doublet separation of the state itself.

The potential curves for the repulsive states *E* and *F* are of course only drawn roughly in Fig. 3, but are so placed that the observed regions of absorption represent the range of most probable transitions.

No theoretical treatment has been given of the electronic states of the fluorides of the heavier metals near the middle of the periodic table. Further experimental data are obviously desirable.

⁵ R. S. Mulliken, Rev. Mod. Phys. 4, 59 (1932).

⁶ See Ferguson, reference 3.

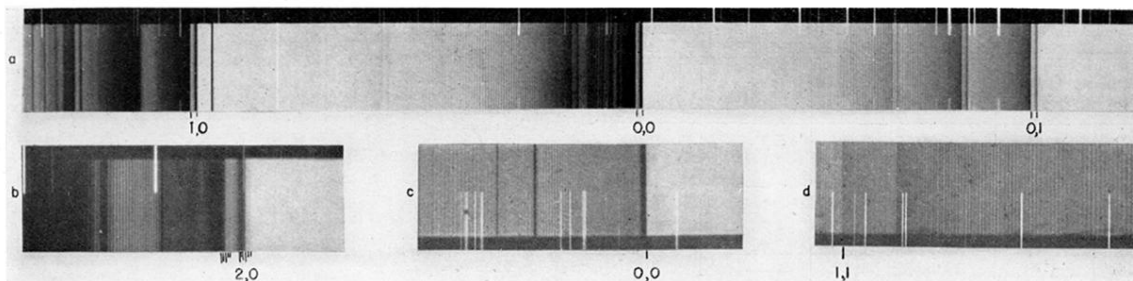


FIG. 2. (a) and (b) ${}^2\Sigma, {}^2\Pi$ system of SnF. (c) ${}^2\Pi, {}^2\Pi$ system of SnF. (d) V, N system of AgCl.